Low-threshold InAs-based interband cascade lasers operating at high temperatures

Lu Li,[1] Yuchao Jiang,[1] Hao Ye,[1] Rui Q. Yang,[1,a)] Tetsuya D. Mishima,[2] Michael B. Santos,[2] and Matthew B. Johnson[2]
[1]*School of Electrical and Computer Engineering, University of Oklahoma, Norman, Oklahoma 73019, USA*
[2]*Homer L. Dodge Department of Physics and Astronomy, University of Oklahoma, Norman, Oklahoma 73019, USA*

(Received 8 April 2015; accepted 15 June 2015; published online 24 June 2015)

InAs-based interband cascade (IC) lasers with improved optical confinement have achieved high-temperature operation with a threshold current density as low as 247 A/cm^2 at 300 K for emission near 4.6 μm. The threshold current density is the lowest ever reported among semiconductor mid-infrared lasers at similar wavelengths. These InAs-based IC devices lased in pulsed mode at temperatures up to 377 K near 5.1 μm. Narrow-ridge devices were able to operate in continuous-wave mode at temperatures up to 308 K near 4.8 μm. The implications and prospects of these results are discussed. © *2015 AIP Publishing LLC*. [http://dx.doi.org/10.1063/1.4922995]

Interband cascade (IC) lasers were projected to be efficient mid-infrared (IR) semiconductor light sources with high voltage efficiency because they utilize type-II heterointerfaces to reuse each injected electron to generate multiple photons based on interband transitions.[1–3] In the last decade, remarkable progress in developing IC lasers on GaSb substrates has been achieved especially in the 3–4 μm wavelength region.[4–12] Low threshold current density (e.g., ~100 A/cm^2 at 3.6 μm) and low power consumption (<0.1 W) at room temperature[4–12] have led to growing applications in chemical sensing, including the detection of CH_4 on Mars.[13] IC lasers with a wavelength coverage extended to 11 μm (Ref. 14) have been developed using InAs substrates[15–20] that allow a plasmon waveguide approach that was initially used in quantum cascade lasers.[21–23] Highly doped n$^+$-InAs layers are used for the plasmon outer cladding layer, instead of the InAs/AlSb superlattice (SL) cladding layers that are used in GaSb-based IC lasers. This results in a significant reduction of strain accumulations and shutter movements during the growth by molecular beam epitaxy (MBE). Additionally, InAs-based IC lasers benefit from the significantly higher thermal conductivity and the substantially lower refractive index of n$^+$-InAs layers compared to InAs/AlSb SL layers.[7,22–24] The refractive index of doped InAs can be evaluated by knowing the plasmon frequency via reflectance measurements[24,25] or calculating the band-structure by a Kane **k**·**p** model that includes the non-parabolic effect.[26–28] Despite these advantages, the continuous wave (cw) operation of InAs-based IC lasers at room temperature had not been demonstrated until this work.

In plasmon waveguide IC lasers, highly doped n$^+$-InAs layers have a high optical absorption loss. To reduce the loss in the waveguide in InAs-based IC lasers that were developed previously, relatively thick (e.g., >1 μm) undoped InAs layers were used as separate confinement layers (SCLs). However, a significant portion of the optical intensity profile is in the thick SCL region (see Fig. 1) and thus the optical confinement factor (Γ) in the center active cascade region is reduced. Consequently, the attainable optical gain is lowered, resulting in a relatively high threshold current density. To improve this, in this work, a semiconductor intermediate cladding layer with a refractive index that is smaller than the refractive index of the center active region is introduced to replace a portion of the SCLs, as shown in Fig. 1. With the insertion of this intermediate (int.) cladding layer between the plasmon cladding and SCLs, the optical wave decays exponentially (i.e., the equivalent wave-vector perpendicular to the layer is imaginary) in the cladding layers in contrast to the propagating wave (i.e., the equivalent wave-vector is real) in SCLs. Thus, the optical wave is squeezed more in the center active region with a significantly enhanced confinement factor (~40% in the example of Fig. 1). As such, the optical modal gain will be increased and the optical intensity in the plasmon outer cladding region (Γ_{OC}) would be reduced (by more than 20% for the example of Fig. 1). Consequently, the laser with intermediate cladding layers

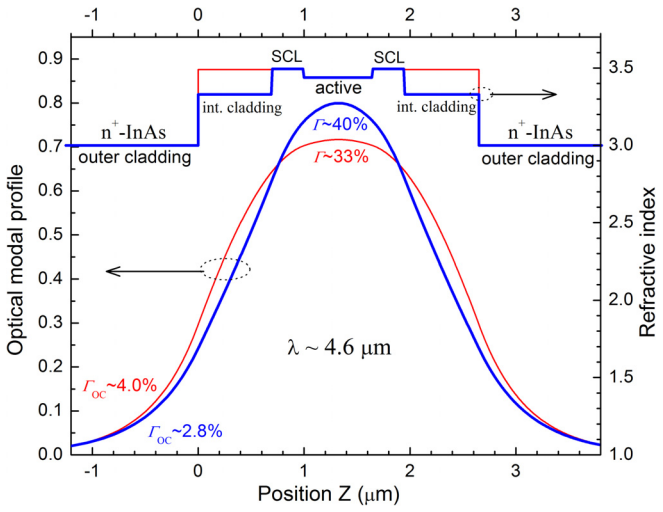

FIG. 1. Calculated optical modal profiles of IC lasers without (thin lines) and with intermediate SL cladding layers (thick lines).

a)Also at Applied Quantum Enovation, Norman, OK 73069, USA. Electronic mail: Rui.Q.Yang@ou.edu

TABLE I. Parameters of wafer structures and pulsed performance features of broad-area devices.

Wafer	No. of stages	Top n^+-InAs layer (nm)	Inter. SL clad. (μm)	InAs SCL (μm)	Doping (cm^{-3}) in e injector	Cavity length (mm)	λ (μm) at 300 K	Lowest J_{th} (A/cm^2) at 300 K	J_{th} (kA/cm^2) at T_{max} (K)
R125	15	35	0	1.5/1.3	3.3×10^{18}	2.0	5.1	393	1.6@340
R136		800	1.0	0.35	3.3×10^{18}	1.5	5.2	340	1.6@360
R140		35		0.35	3.3×10^{18}	2.0	4.6	247	2.0@370
R142	12	700		0.39	3.3×10^{18}	2.0	4.75	290	1.8@359
R143		700		0.39	1.6×10^{18}	2.0	4.5	278	3.9@376
R144	10	800		0.43	3.3×10^{18}	2.0	4.7	290	3.1@377
R145		800		0.43	1.6×10^{18}	2.0	4.6	330	2.0@360

can have a lower optical loss and a lower threshold current density, resulting in significantly improved device performance.

IC laser structures were designed with symmetrical intermediate cladding layers and SCLs, then grown on *n*-type InAs substrates in a Gen-II MBE system. Their structural parameters (and key performance features as discussed later) are shown in Table I with a varied number of cascade stages and SCL thicknesses. These IC lasers have their cascade regions similar to that in Refs. 17 and 18 with some small adjustments in layer thicknesses for tuning the lasing wavelength according to variations in MBE system conditions. The calculated band-edge diagram (based on a two-band model[27,28]) with a detailed layer sequence for one cascade stage is shown in Fig. 2. The central 3 InAs quantum wells (QWs) in the electron injector of each cascade stage were doped with Si to 3.3×10^{18} or $1.6 \times 10^{18}\,cm^{-3}$ to explore how the carrier-rebalancing[6] works in InAs-based IC lasers. The intermediate cladding layer was a 25 Å/23 Å InAs/AlSb SL, in which each AlSb layer contains a 3 Å-thick AlAs interface for achieving strain balance. A digitally graded InAs/AlSb(As) QW region was inserted as a transition/connection bridge between the SL intermediate cladding layers and other regions for smoothing carrier transport, similar to GaSb-based IC lasers.[7–9] This thin (~58 nm) transition region is grouped into the SL intermediate cladding layer thickness listed in Table I. It should be noted that the intermediate claddings (1.0 μm thick) are substantially thinner than a regular SL cladding layer (2–3 μm thick) used in GaSb-based IC lasers. Hence, the thermal resistance of InAs-based IC lasers with the SL intermediate cladding layers should in principle be lower than that of GaSb-based IC lasers. Table I also includes an IC laser wafer, R125, without intermediate cladding layers for comparison. Wafer R125 was grown earlier with bottom and top SCLs that are relatively thick and have different thicknesses.

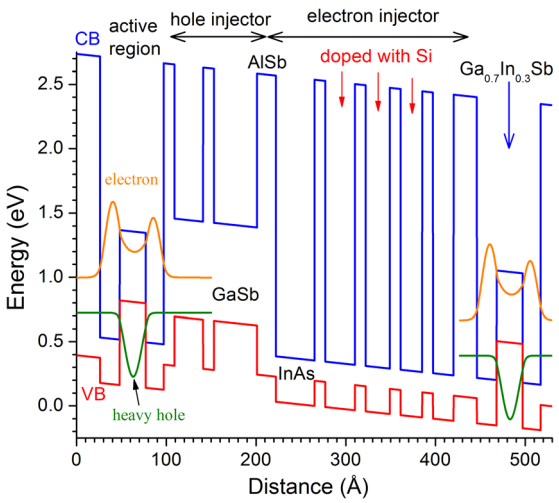

FIG. 2. Calculated band-edge diagram of one cascade stage and the layer sequence. The layer thickness (in unit of Å) of each layer in one IC stage beginning at the barrier separating the electron injector and the active region is 26, 22, 29, 20, 12, 32, 12, 48, 21, 43, 12, 33, 12, 27, 12, 24, 12, and 23. The structure was designed to lase at a wavelength of 4.6 μm at room temperature.

The laser wafers were processed into deep-etched broad-area (150- and 100-μm-wide) mesa stripe lasers and narrow-ridge (10-, 12-, 15-, and 20-μm-wide) lasers by contact photolithography and wet chemical etching. The processed wafers were typically cleaved into laser bars with lengths from 1.5 to 2.0 mm (unless otherwise specified) and the facets were left uncoated. The laser bars were mounted epilayer side up on copper heat sinks with indium solder, and placed on the cold finger of a cryostat for measurements in cw and pulsed modes. In pulsed measurements, the applied current pulse width was 1 μs at a repetition rate of 5 kHz. When the applied current was larger than 1 A, the pulse width was reduced to 250 ns to avoid possible Joule heating.

In pulsed operation, broad-area (BA) devices made from IC laser wafers with intermediate SL cladding layers exhibited substantially higher operating temperatures and lower threshold current densities compared to BA devices made from wafer R125 without the intermediate SL cladding layers, as summarized in Table I. For example, a BA device from a 15-stage wafer R140 had a threshold current density J_{th} of 247 A/cm^2 near 4.6 μm at 300 K, the lowest ever reported among mid-IR semiconductor lasers at similar wavelengths. Another BA device from a 10-stage wafer R144 lased at temperatures up to 377 K near 5.1 μm, as shown in Fig. 3, the highest operating temperature reported for electrically pumped interband lasers at this wavelength. In Fig. 4, threshold current densities for several representative devices made from 12-stage and 10-stage wafers are plotted as a function of the heat-sink temperature, *T*. The characteristic temperature, T_0 (~46–57 K in the neighborhood of 300 K), is comparable to that of state-of-the-art GaSb-based IC lasers in the 3–4 μm wavelength region.[12] However, the performance features of the BA devices presented in Table I and Fig. 4 do not provide clear indications of how the threshold current density would change with the number of cascade stages and the doping concentration in

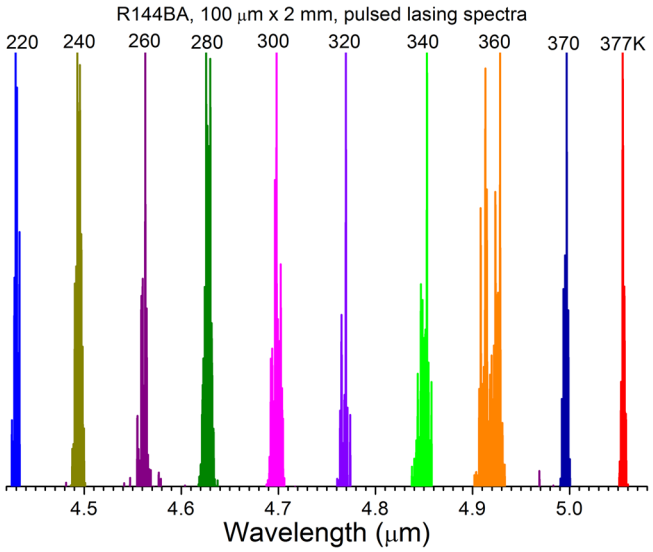

FIG. 3. Near threshold pulsed lasing spectra of 100-μm-wide devices from wafer R144.

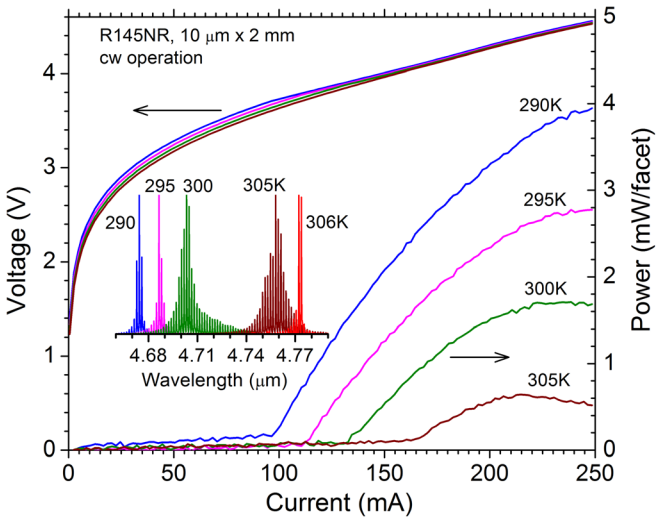

FIG. 5. Current-voltage-light characteristics for a 10-μm-wide, 2-mm-long device (from wafer R145) in cw operation. The inset is the cw lasing spectra at several heat-sink temperatures of 290 to 306 K.

the electron injectors. This may be attributed to variations of material quality and uniformity. The IC laser structures with intermediate SL cladding layers were grown soon after the MBE chamber was serviced and their material quality was not as good as in the previous growth campaign (e.g., wafer R125). Nevertheless, it is very evident that the lasers made from the later wafers exhibited significantly improved device performance, which validates the projection from our waveguide modeling shown in Fig. 1.

Narrow-ridge (NR) devices (from 10- and 12-stage wafers) with a top layer of ~4-μm electroplated gold were able to lase in cw mode at room temperature and above at wavelengths from 4.6 to 4.9 μm, as indicated in Fig. 4. The cw operating temperatures achieved by the 10-stage lasers were higher than those of the 12-stage lasers as the required operating voltage was lower in 10-stage lasers. Figure 5 shows the cw current-voltage-light (*I-V-L*) characteristics and lasing spectra of a 10-μm-wide and 2-mm-long device (from wafer R145) at several heat-sink temperatures. The Joule heating in the laser was substantial at 300 K and above,

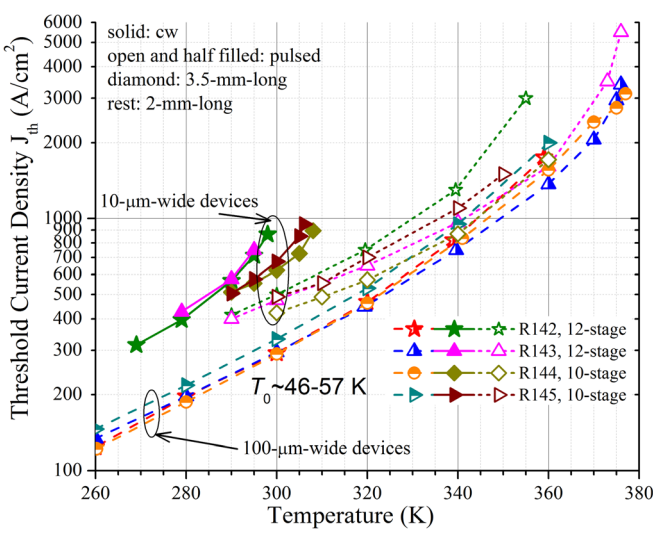

FIG. 4. Threshold current density, J_{th} vs. heat-sink temperature, T, for both BA and NR lasers made from 10-stage and 12-stage wafers.

as reflected in Fig. 5, which shows the thermal rollover and substantial red shifts of the lasing wavelength. Nevertheless, the detected output power exceeded 1.6 mW/facet at 300 K without accounting for beam divergence loss. The input power at threshold was slightly less than 0.52 W at 300 K, which is higher than the state-of-the-art GaSb IC lasers in the 3–4 μm wavelength region,[12] but this is still encouraging considering that the lasing was at a longer wavelength from a wafer of the initial attempt with intermediate SL cladding layers on InAs substrates. Another 10-stage NR device (from wafer R144) with a long cavity (3.5 mm) lased in cw mode at temperatures up to 308 K near 4.85 μm, as shown in Fig. 6. The attainable output power was higher from this long cavity laser and did not exhibit thermal rollover at the maximum injection current (350 mA) that was applied to the device. The cw operation of these InAs-based IC lasers was affected by their relatively high thermal resistance, which limited the maximum allowed cw threshold current density below 1 kA/cm^2, as shown in Fig. 4. By comparing threshold

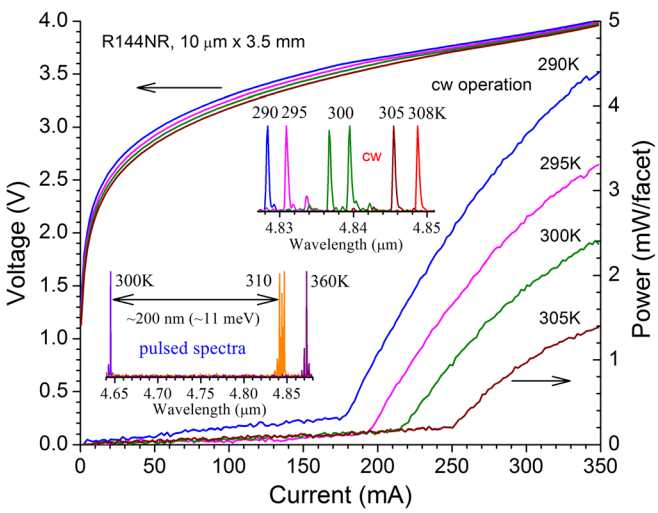

FIG. 6. Current-voltage-light characteristics for a 10-μm-wide, 3.5-mm-long device (from wafer R144) in cw operation. One inset shows the cw lasing spectra at several heat-sink temperatures of 290 to 308 K. The other inset shows the pulsed lasing spectra at 300, 310, and 360 K.

current densities in cw and pulsed modes, the specific thermal resistance for the 10-μm-wide ridge lasers was deduced to be in the range of 6.5–11 K cm^2/kW, which is higher than the reported value (5.4 K cm^2/kW) for a 12-stage 10-μm-wide ridge IC laser with a similar layer structure and thicker SL cladding layers.[4] This suggests that there is still room for improving thermal dissipation of these InAs-based IC lasers even without employing epilayer-down mounting.

In pulsed mode, the narrow-ridge devices lased at temperatures up to 376 K, which is comparable to BA devices. However, their threshold current densities were generally higher than corresponding values for broad-area lasers at temperatures below 320 K, as shown in Fig. 4. Differences were more evident at lower temperatures. For example, at 300 K, the pulsed threshold current density in a 10–μm-wide narrow-ridge device was about 45%–71% higher than that in a broad-area laser at the same cavity length. The difference is substantially higher than the ~21% difference reported for IC lasers in the 3–4 μm wavelength region.[5] This suggests a somewhat significant current leakage from the sidewalls due to imperfect passivation, which implies further room to achieve better performance by reducing this surface leakage. Another behavior that was observed from a NR device was a substantial mode hopping (~200 nm in wavelength or ~11 meV in transition energy, which is within the width of a typical material gain peak (>20 meV)) when the temperature was changed from 300 to 310 K, as shown in the inset of Fig. 6. This type of mode hopping was not observed from BA devices (e.g., Fig. 3) made from the same wafer. Hence, material non-uniformity may be one of several possible factors causing the mode hopping.

In summary, InAs-based IC lasers were demonstrated with low threshold current densities and cw operation at room temperature. This progress was enabled by the use of intermediate SL cladding layers for enhancing optical confinement and reducing internal absorption loss. Further advancements, including extension of room-temperature cw operation to longer wavelengths, are expected with improvements in material quality and device fabrication, as well as optimization of device design that includes further examination of carrier-rebalancing approach with different doping concentrations. In principle, the intermediate cladding layers can also be used to improve the performance of InAs-based intersubband quantum cascade lasers,[29] which are based on transverse magnetic (TM) modes instead of the transverse electric (TE) modes of IC lasers.

This work was partially supported by the National Science Foundation (IIP-1346307).

[1]R. Q. Yang, "Infrared laser based on intersubband transitions in quantum wells," at *7th International Conference on Superlattices, Microstructures and Microdevices*, Banff, Canada, August, 1994 [Superlattices Microstructures **17**, 77 (1995)].
[2]J. R. Meyer, I. Vurgaftman, R. Q. Yang, and L. R. Ram-Mohan, "Type-II and type-I interband cascade lasers," Electron. Lett. **32**, 45 (1996).
[3]R. Q. Yang and S. S. Pei, "Novel type-II quantum cascade lasers," J. Appl. Phys. **79**, 8197 (1996).
[4]K. Mansour, Y. Qiu, C. J. Hill, A. Soibel, and R. Q. Yang, "Mid-IR interband cascade lasers at thermoelectric cooler temperatures," Electron. Lett. **42**, 1034 (2006).
[5]W. W. Bewley, C. L. Canedy, C. S. Kim, M. Kim, J. R. Lindle, J. Abell, I. Vurgaftman, and J. R. Meyer, "Ridge-width dependence of midinfrared interband cascade laser characteristics," Opt. Eng. **49**, 111116 (2010).
[6]I. Vurgaftman, W. W. Bewley, C. L. Canedy, C. S. Kim, M. Kim, C. D. Merritt, J. Abell, J. R. Lindle, and J. R. Meyer, "Rebalancing of internally generated carriers for mid-infrared interband cascade lasers with very low power consumption," Nat. Commun. **2**, 585 (2011).
[7]R. Q. Yang, "Interband cascade (IC) lasers," in *Semiconductor Lasers: Fundamentals and Applications*, edited by A. Baranov and E. Tournie (Woodhead Publishing Limited, Cambridge, UK, 2013), Chap. 12, and references therein.
[8]I. Vurgaftman, W. W. Bewley, C. L. Canedy, C. S. Kim, M. Kim, C. D. Merritt, J. Abell, and J. R. Meyer, "Interband cascade lasers with low threshold powers and high output powers," IEEE J. Sel. Top. Quantum Electron. **19**, 1200210 (2013), and references therein.
[9]R. Weih, M. Kamp, and S. Höfling, "Interband cascade lasers with room temperature threshold current densities below 100 A/cm^2," Appl. Phys. Lett. **102**, 231123 (2013).
[10]C. L. Canedy, J. Abell, C. D. Merritt, W. W. Bewley, C. S. Kim, M. Kim, I. Vurgaftman, and J. R. Meyer, "Pulsed and CW performance of 7-stage interband cascade lasers," Opt. Express **22**, 7702 (2014).
[11]L. Shterengas, R. Liang, G. Kipshidze, T. Hosoda, G. Belenky, S. S. Bowman, and R. L. Tober, "Cascade type-I quantum well diode lasers emitting 960 mW near 3 μm," Appl. Phys. Lett. **105**, 161112 (2014).
[12]I. Vurgaftman, R. Weih, M. Kamp, J. R. Meyer, C. L. Canedy, C. S. Kim, M. Kim, W. W. Bewley, C. D. Merritt, J. Abell, and S. Höfling, "Interband cascade lasers," J. Phys. D: Appl. Phys. **48**, 123001 (2015).
[13]C. R. Webster, P. R. Mahaffy, S. K. Atreya, G. J. Flesch, M. A. Mischna, P.-Y. Meslin, K. A. Farley, P. G. Conrad, L. E. Christensen, A. A. Pavlov *et al.*, "Mars methane detection and variability at Gale crater," Science **347**, 415 (2015).
[14]L. Li, H. Ye, Y. Jiang, R. Q. Yang, J. C. Keay, T. D. Mishima, M. B. Santos, and M. B. Johnson, "MBE-grown long-wavelength interband cascade lasers on InAs substrates," J. Cryst. Growth **425**, 369 (2015).
[15]Z. Tian, R. Q. Yang, T. D. Mishima, M. B. Santos, R. T. Hinkey, M. E. Curtis, and M. B. Johnson, "InAs-based interband cascade lasers near 6 μm," Electron. Lett. **45**, 48 (2009).
[16]Z. Tian, L. Li, Y. Hao, R. Q. Yang, T. D. Mishima, M. B. Santos, and M. B. Johnson, "InAs-based interband cascade lasers with emission wavelength at 10.4 μm," Electron. Lett. **48**, 113 (2012).
[17]Z. Tian, Y. Jiang, L. Li, R. T. Hinkey, Z. Yin, R. Q. Yang, T. D. Mishima, M. B. Santos, and M. B. Johnson, "InAs-based interband cascade lasers near 5.3 μm," IEEE J. Quantum Electron. **48**, 915 (2012).
[18]R. Q. Yang, L. Li, L. Zhao, Y. Jiang, Z. Tian, H. Ye, R. T. Hinkey, C. Niu, T. D. Mishima, M. B. Santos, J. C. Keay, M. B. Johnson, and K. Mansour, "Recent progress in development of InAs-based interband cascade lasers," Proc. SPIE **8640**, 86400Q (2013).
[19]M. Dallner, S. Höfling, and M. Kamp, "Room-temperature operation of InAs-based interband-cascade-lasers beyond 6 μm," Electron. Lett. **49**, 286 (2013).
[20]M. Dallner, F. Hau, S. Höfling, and M. Kamp, "InAs-based interband-cascade-lasers emitting around 7 μm with threshold current densities below 1 kA/cm^2 at room temperature," Appl. Phys. Lett. **106**, 041108 (2015).
[21]C. Sirtori, J. Faist, F. Capasso, D. L. Sivco, A. L. Hutchinson, and A. Y. Cho, "Continuous wave operation of midinfrared (7.4–8.6 μm) quantum cascade lasers up to 110 K temperature," Appl. Phys. Lett. **68**, 1745 (1996).
[22]K. Ohtani and H. Ohno, "An InAs-based intersubband quantum cascade laser," Jpn. J. Appl. Phys., Part 2 **41**, L1279 (2002).
[23]R. Teissier, D. Barate, A. Vicet, C. Alibert, A. N. Baranov, X. Marcadet, C. Renard, M. Garcia, C. Sirtori, D. Revin, and J. Cockburn, "Room temperature operation of InAs/AlSb quantum cascade lasers," Appl. Phys. Lett. **85**, 167 (2004).
[24]R. T. Hinkey, Z. Tian, R. Q. Yang, T. D. Mishima, and M. B. Santos, "Reflectance spectrum of plasmon waveguide interband cascade lasers and observation of the Berreman effect," J. Appl. Phys. **110**, 043113 (2011).
[25]Y. B. Li, R. A. Stradling, T. Knight, J. R. Birch, R. H. Thomas, C. C. Phillips, and I. T. Ferguson, "Infrared reflection and transmission of undoped and Si-doped InAs grown on GaAs by molecular beam epitaxy," Semicond. Sci. Technol. **8**, 101 (1993).
[26]E. O. Kane, "The ***k•p*** method," in *Physics of III-V Compounds*, Semiconductors and Semimetals, Vol. 1, edited by R. K. Willardson and A. C. Beer (Academic, New York, 1966), p. 75.
[27]R. Q. Yang and J. M. Xu, "Analysis of transmission in polytype interband tunneling heterostructures," J. Appl. Phys. **72**, 4714 (1992).
[28]R. Q. Yang and J. M. Xu, "Bound and quasibound states in leaky quantum wells," Phys. Rev. B **46**, 6969 (1992).
[29]R. Q. Yang, "InAs-based quantum cascade lasers with enhanced confinement" ~~(unpublished)~~.